Peeling characteristics of the tarsometatarsal bones and influencing factors for chicken feet peeling

Dongming Gao, Leyuan Wang, Wenyuan Xu, Zongqiang Fu*

(*School of Computer and Artificial Intelligence, Beijing Technology and Business University, Beijing 100048, China*)

Abstract: The process of deboning chicken feet has a significant impact on the quality and taste of chicken feet products. However, comprehensive models for its mechanical properties, particularly in terms of peel strength, are lacking. A TPA-based model for peel strength and related texture indicators, including hardness, chewiness, springiness, and adhesiveness, was developed, enabling comprehensive characterization of the mechanical behavior of chicken feet during the deboning process. Regression analysis and MATLAB-based grid search were used to optimize cooling temperature, heating time, and heating temperature, with peel strength as the main constraint. The optimal condition was identified as cooling at 5.0°C, heating for 8.00 min, and heating at 89.0°C. This study provides a quantitative optimization framework that integrates mechanical properties with texture evaluation, enabling precise control of deboning efficiency and product quality. The proposed method improves processing stability and offers a transferable modeling approach for other collagen-rich food materials in food engineering applications.

Keywords: chicken feet, peel strength, texture profile analysis, parameter optimization, food engineering

DOI: 10.25165/j.ijabe.20261903.9626

Citation: Gao D M, Wang L Y, Xu W Y, Fu Z Q. Peeling characteristics of the tarsometatarsal bones and influencing factors for chicken feet peeling. Int J Agric & Biol Eng, 2026; 19(3): 42–49.

1 Introduction

Chicken feet are widely used as a food ingredient in the food industry. In countries such as China, chicken feet are often turned into snack foods with high commercial value[1-3]. This transformation of chicken feet into snack foods not only allows for their global distribution but also increases profitability in the poultry slaughter industry and helps reduce food waste[4-6]. In current industrial practice, deboning is a key step that directly determines processing efficiency and product classification, and it is closely related to the stability of product quality and consumer acceptance. The deboning process is a crucial technological step for large-scale production, and the quality and eating experience of chicken feet products are strongly influenced by this process[7]. Chicken feet are made up of tarsometatarsal and phalange bones, with the tarsometatarsal segment serving as the primary support system for the entire leg. This segment plays a crucial role in providing essential functions such as impact resistance and stability. Because of these structural functions, the tarsometatarsal bones experience complex loading conditions and deformation modes during processing. The muscular and ligamentous structures within the chicken feet tarsometatarsal bones are complex and well developed and significantly affect the deboning process[8].

The chicken feet tarsometatarsal bones can be divided into anterior, middle, and posterior segments. Owing to the irregular morphology and abundant soft tissues in the anterior and posterior regions, their mechanical properties are relatively complex and unstable[9]. Previous studies have shown that the three segments exhibit similar changes in mechanical performance and product texture under different treatment conditions[10]. However, most studies have focused on overall mechanical behavior or macroscopic texture changes, whereas systematic quantitative characterization of peel strength and related mechanical parameters in specific segments remains limited. In chicken feet pretreatment, springiness, adhesiveness, hardness, and chewiness are important but distinct texture indicators[11-13]. Furthermore, the relationships between internal mechanical properties and texture under different treatment conditions remain unclear, and models that simultaneously characterize peel strength and texture indicators for process optimization are still lacking.

Texture profile analysis (TPA) is widely used to quantify texture attributes such as hardness, springiness, adhesiveness, and chewiness in food matrices, providing a useful mechanical–sensory framework for collagen-rich tissues such as chicken feet. By establishing regression relationships between process parameters and TPA indicators, changes in internal structure and mouthfeel under different treatment conditions can be described within a unified mechanical framework. Grid-based search is an effective approach for identifying optimal parameter combinations in a predefined space. Therefore, combining a TPA-based model with a grid-based search strategy provides a quantitative route for integrating mechanical properties, texture evaluation, and process constraints such as peel strength.

This study focuses on the midsection of chicken feet tarsometatarsal bones and uses a grid-based search to optimize processing parameters under peel-strength constraints while preserving desirable texture. The objective was to reduce peel strength, improve deboning efficiency, and maintain favorable textural properties. The results provide a quantitative basis for process optimization in chicken feet processing and may also serve

Received date: 2024-12-20 **Accepted date:** 2026-06-01

Biographies: Dongming Gao, PhD, Associate Professor, research interest: intelligent agricultural equipment and technology, Email: gaodongming@btbu.edu.cn; **Leyuan Wang**, Postgraduate, research interest: intelligent agricultural equipment and technology, Email: wangleleyuan@163.com; **Wenyuan Xu**, Master, research interest: food machinery, Email: 894491834@qq.com.

***Corresponding author: Zongqiang Fu**, PhD, Associate Professor, research interest: food machinery, Beijing Technology and Business University, Beijing 100048, China. Email: fuzongqiang@btbu.edu.cn.

as a reference for other collagen-rich food materials.

Compared with previous studies that mainly described overall mechanical behavior or macroscopic texture changes[14–16], this study emphasizes the quantitative coupling of peel strength and TPA indicators in the midsection of chicken feet tarsometatarsal bones, thereby providing a more direct basis for deboning-oriented process optimization.

2 Materials and methods

2.1 Materials

Chicken feet of uniform size and without visible damage were purchased from Wumart Commercial Group Co. (Beijing, China) and used as the raw materials in this study. After purchase, the samples were immediately transported to the laboratory under refrigerated conditions and stored at 4°C prior to use. All samples were processed within 24 h to minimize variations in physicochemical and mechanical properties. Sodium chloride (NaCl) and rhodamine B were purchased from Solarbio Biotechnology Co. (Beijing, China).

2.2 Pretreatment

The chicken feet samples were thawed to room temperature, cleaned by removing surface dirt, and rinsed with water. On the basis of a single-factor experiment, three factors, namely, the heating temperature, heating time, and cooling temperature, were identified as influencing factors[17].

Research has indicated that once the cooling time of chicken feet reaches the protein cooling stabilization time, further cooling does not significantly affect the quality or processing but affects only the efficiency. Therefore, the treated chicken feet were cooled to the protein cooling stabilization time before the tests were conducted. Different treatment conditions for chicken feet were applied according to the experimental design scheme generated by the Central Composite Design (CCD) tool in Design Expert 8.0, and the treated samples were prepared for further testing, including TPA and peel test as shown in Figure 1.

2.3 TPA

TPA experiments were conducted using a texture analyzer (TMS-Pilot, Food Technology Corporation, USA) equipped with a 500 N load cell (ILC 500N). A flat cylindrical probe (P/5) was used for all measurements. The instrument was calibrated prior to testing according to the manufacturer's instructions. The following test conditions were used: pretest speed, 1.00 mm/s; test speed, 2.00 mm/s; posttest speed, 5.00 mm/s; target mode, 50%; and trigger force, 5.0 g. For the experiment, samples from the midsection of tarsometatarsal bones on the posterior side of the chicken feet were selected and cut into square pieces measuring 5 mm×5 mm. The TPA parameters measured included hardness, springiness, adhesiveness, and chewiness[18–20]. These parameters were calculated on the basis of the recorded curves. All measurements were performed twice at different locations on each tissue, and the average values were calculated[21].

2.4 Peel test

In the chicken foot peel test, the first step involved removing the skin and toe bones. Next, two reference lines were drawn 25 mm apart on the lateral side of the tarsometatarsal bones. The chicken feet were then cut open along these lines to create peel test samples. A specific length of pre-peeling treatment was applied to facilitate clamping. A hinged-clamping fixture was used to grip the samples, ensuring alignment of the peel force with the axis of the tarsometatarsal bones. This involved opening a small hole with a diameter of 3 mm at one end of the tarsometatarsal bones and fixing one end of the sample through the hole. The other end of the sample was clamped in a custom-made fixture to ensure firmness and even distribution of the applied tensile force across the width of the sample[15,16,22]. Peel force measurements were conducted via a TMS-Pilot texture analyzer, with the samples separated at a constant rate of 100 mm/min, resulting in a 180° peel angle between the skin and bones until complete detachment of the sample. The sampling frequency of the texture analyzer during the experiment was set at 1000 Hz. To ensure that the experimental results are not affected by sample breakage, the peel strength should be lower than the maximum equivalent tensile strength[16,22–24]. The formula for calculating the equivalent tensile strength ($E\sigma_c$) is provided by Equation (1):

$$E\sigma_c = \frac{F_m}{L_b} \tag{1}$$

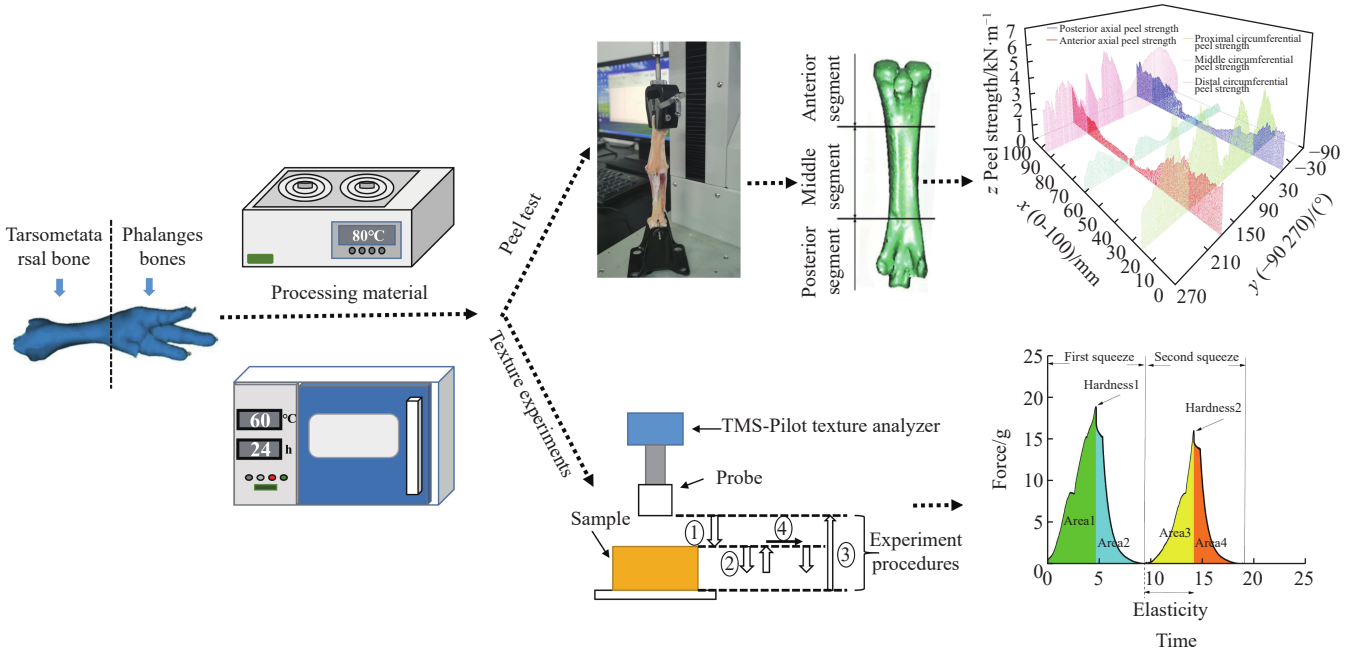

Figure 1 Experimental procedure

where, $E\sigma_c$ is the equivalent tensile strength, N/m; F_m is the maximum load, N; and L_b is the sample width, m.

2.5 Grid search

The search ranges and step sizes for cooling temperature, heating time, and heating temperature were determined according to the experimental requirements. A parameter grid containing all possible combinations was then generated using the mesh grid function, and the corresponding response values for hardness, springiness, adhesiveness, chewiness, and peel strength were calculated from the regression equations for each parameter combination. Peel strength was used as a constraint to screen the combinations, and a weighted sum of the response values was calculated to obtain the overall score. Combinations that did not satisfy the constraint were excluded by assigning negative infinity to their scores. The parameter combination that satisfied the constraint and yielded the highest score was identified, and all combinations with scores greater than or equal to 20, together with the corresponding cooling temperature, heating time, and heating temperature, were output to determine the parameter ranges[25–27].

2.6 Fluorescence imaging analysis

After processing, the chicken feet were sliced into pieces. A sample with dimensions of approximately 10×10×3 mm and a smooth surface (necessary for visualization by CLSM) was carefully removed via a microtome blade. The sample was then placed in physiological saline (0.154 mol/L NaCl) containing rhodamine B (0.4 mg/mL) and left undisturbed for 90-120 min to allow for staining.

2.7 Experimental design and data analysis

This study focused on three main factors: heating temperature, heating time, and cooling temperature. A central composite design (CCD) with a 3-factor, 3-level arrangement was used to construct the experimental plan, with response surface analysis software applied for design implementation. The levels of the factors are outlined in Table 1, which includes a total of 17 experimental runs. In Table 1, A represents the heating temperatures of 80.0°C, 87.5°C, and 95.0°C. B represents heating times of 5.00 min, 10.50 min, and 16.00 min. C represents the cooling temperature at 0.0°C, 10.5°C, or 25.0°C. The alpha values indicate the level of the factors at the center point.

Table 1 Corresponding actual values of the factors tested in the central composite design

Factor name	–1	+1	–alpha	+alpha
A: Heating temperature/°C	80.0	95.0	74.886 550	100.113 400
B: Heating time/min	5.00	16.00	1.250 139	19.749 860
C: Cooling temperature/°C	0.0	25.0	–8.522 410	33.522 410

Note: alpha=1.681 79.

The data collected in this study were obtained through multiple measurements, with each measurement being conducted in triplicate or more. The average values were then calculated from these measurements. Both positive and negative standard deviations were determined, with error bars used for data representation.

Statistical analysis of the experimental results was performed using Design-Expert 8.0 to evaluate the effects of treatment conditions on the experimental indicators and to establish predictive models. Grid search was subsequently used for parameter optimization in the midsection of chicken feet tarsometatarsal bones, with peel strength as a constraint. Weight coefficients were introduced to calculate the total scores, reflecting the relative importance of each TPA indicator[28,29]. Parameter combinations satisfying the constraint were identified according to the score range. Response surface and contour analyses were further conducted to visualize the effects of treatment conditions on the experimental indicators and to determine the optimal treatment range.

3 Results and discussions

3.1 TPA

The results of the TPA experiment based on the central composite design are summarized in Table 2. Different treatment conditions produced clear variations in springiness, hardness, adhesiveness, and chewiness.

Table 2 Results of the TPA texture experiment of the central composite design

Run	A: Heating temperature/°C	B: Heating time/min	C: Cooling temperature/°C	Springiness/mm	Hardness/N	Adhesiveness/N	Chewiness/mJ
1	95.0	5.00	25.0	3.242	16.412	10.658	41.607
2	87.5	1.25	12.5	2.428	9.996	6.079	13.626
3	87.5	10.50	33.5	2.995	9.749	14.042	55.586
4	95.0	5.00	0.0	3.278	13.308	8.345	27.357
5	95.0	16.00	25.0	3.245	4.302	2.803	9.096
6	74.9	10.50	12.5	3.606	10.940	7.212	25.970
7	87.5	10.50	12.5	4.182	12.394	10.182	42.576
8	80.0	5.00	0.0	2.156	8.078	3.428	6.785
9	95.0	16.00	0.0	3.611	8.543	5.936	21.436
10	87.5	10.50	12.5	4.174	14.087	10.792	45.044
11	87.5	10.50	-8.5	2.566	29.523	6.950	15.047
12	80.0	16.00	25.0	3.992	15.691	10.757	29.582
13	87.5	19.75	12.5	3.749	8.078	4.508	17.125
14	80.0	5.00	25.0	3.205	17.736	10.719	34.305
15	80.0	16.00	0.0	2.818	9.532	6.278	17.697
16	100.1	10.50	12.5	3.816	8.093	5.600	20.804
17	87.5	10.50	12.5	3.882	15.541	11.392	44.220

Overall, the textural indicators varied markedly under different treatment conditions. These changes were likely associated with heating- and cooling-induced alterations in the protein network and tissue structure[30,31]. Heating may promote protein denaturation and aggregation, thereby affecting hardness and related texture attributes[32,33]. Cooling may also influence moisture redistribution and structural reorganization, which contribute to changes in adhesiveness[34–36]. Chewiness was likewise affected by the combined

variation in other texture attributes under different treatment conditions[37]. Heating temperature, heating time, and cooling temperature all affected the textural properties of chicken feet. Higher heating temperature and prolonged heating time tended to increase hardness, adhesiveness, and chewiness, whereas shorter heating time was more favorable for retaining springiness. Cooling temperature also played an important role in determining the final texture characteristics.

The results of the analysis of variance are presented in Table 3. The regression models for hardness, springiness, adhesiveness, and chewiness were all significant. Among the three factors, cooling temperature showed the most consistent and significant effect on all four TPA indicators, whereas heating time significantly affected hardness, springiness, and adhesiveness. By comparison, the effect of heating temperature was relatively limited. Several interaction and quadratic terms were also significant, suggesting that the effects of processing conditions on texture were not simply linear.

The regression models showed acceptable goodness of fit. The R^2 values for hardness, springiness, adhesiveness, and chewiness were 0.9646, 0.9582, 0.9739, and 0.9113, respectively, and the corresponding adjusted R^2 values were 0.9056, 0.9044, 0.9404, and 0.7972.

As shown in Figure 2, the residuals exhibited no obvious systematic deviation, indicating that the regression assumptions were generally satisfied. In addition, Figure 3 shows good agreement between the predicted and experimental values, supporting the suitability of the developed models for describing the TPA responses of the midsection of chicken feet tarsometatarsal bones.

The regression coefficients describing the relationships between the process variables and the TPA indices are summarized in Table 4.

The change in peel strength is primarily attributed to thermal denaturation. Meanwhile, the changes in hardness, adhesiveness, and chewiness are likely associated with heating- and cooling-induced alterations in the protein network and tissue structure of chicken feet. Heating may promote protein denaturation and aggregation, whereas cooling may influence moisture redistribution and structural reorganization, thereby jointly affecting textural properties. These results provide a quantitative basis for subsequent optimization of deboning-related processing conditions[32,34-36].

3.2 Peel test

The results of the peel test on the midsection of chicken feet tarsometatarsal bones are presented in Table 5, with peel strength values ranging from 0.519 kN/m to 2.252 kN/m.

Higher heating temperatures, such as 95.0°C, could cause significant tissue denaturation, resulting in increased peel strength. On the other hand, lower heating temperatures, such as 80.0°C, may lead to insufficient denaturation and lower peel strength. Importantly, optimal heating times, such as 10.50 min, could ensure sufficient tissue denaturation and increase peel strength. Conversely, short heating times, such as 1.25 min, may result in decreased peel strength due to insufficient denaturation. Additionally, appropriate cooling temperatures, such as 12.5°C, could facilitate tissue recrystallization and increase peel strength. However, higher cooling temperatures, such as 25.0°C, may impede complete structural recovery, leading to decreased peel strength.

On the basis of the analysis of variance (ANOVA) results for peel strength (Table 6), the overall regression model significantly explained peel strength. The sum of squares for the heating temperature is 0.48 with 1 degree of freedom, a mean square of 0.480, and an F-value of 19.31, indicating a significance level of 0.0007. For heating time, the sum of squares is 0.30, with 1 degree of freedom, a mean square of 0.300, and an F-value of 12.25, indicating a significance level of 0.0039. The sum of squares for the cooling temperature is 3.68, with 1 degree of freedom, a mean square of 3.680, and an F-value of 148.44, indicating a significance level of less than 0.0001. These results indicate that the heating temperature, heating time, and cooling temperature significantly

Table 3 Analysis of variance results

Source	Indicator	Sum of squares	Degrees of freedom	Mean square	F-value	Significance
Model	Hardness	503.10	10	50.31	16.34	0.0014
	Springiness	5.67	9	0.63	17.81	0.0005
	Adhesiveness	157.05	9	17.45	29.07	<0.0001
	Chewiness	329.69	9	329.60	7.99	0.0060
A: Heating temperature (°C)	Hardness	12.88	1	12.88	4.18	0.0868
	Springiness	0.18	1	0.18	5.02	0.0601
	Adhesiveness	2.77	1	2.77	4.61	0.0688
	Chewiness	0.44	1	0.44	0.011	0.9210
B: Heating time (min)	Hardness	31.36	1	31.36	10.18	0.0188
	Springiness	1.18	1	0.18	33.22	0.0007
	Adhesiveness	7.35	1	2.77	12.24	0.0100
	Chewiness	50.87	1	0.44	1.23	0.3036
C: Cooling temperature (°C)	Hardness	195.50	1	195.50	63.50	0.0002
	Springiness	0.47	1	0.47	13.35	0.0081
	Adhesiveness	38.32	1	38.32	63.85	<0.0001
	Chewiness	877.85	1	877.85	21.27	0.0025
AB	Hardness	33.14	1	33.14	10.77	0.0168
	Springiness	0.15	1	0.15	4.37	0.0748
	Adhesiveness	21.63	1	21.63	36.03	0.0005
	Chewiness	248.88	1	248.88	6.03	0.0438
AC	Hardness	35.93	1	35.93	11.67	0.0142
	Springiness	0.86	1	0.86	24.35	0.0017
	Adhesiveness	19.81	1	19.81	33.01	0.0007
	Chewiness	175.73	1	175.73	4.26	0.0780
BC	Hardness	14.70	1	14.70	4.77	0.0716
	Springiness	5.289×10^{-3}	1	5.289×10^{-3}	0.15	0.7105
	Adhesiveness	8.52	1	8.52	14.20	0.0070
	Chewiness	222.88	1	222.88	5.40	0.0531
A^2	Hardness	36.49	1	36.49	11.85	0.0138
	Springiness	0.16	1	0.16	4.45	0.0728
	Adhesiveness	25.75	1	25.75	42.90	0.0003
	Chewiness	597.18	1	597.18	14.47	0.0067
B^2	Hardness	43.69	1	43.69	14.19	0.0093
	Springiness	1.29	1	1.29	36.45	0.0005
	Adhesiveness	40.90	1	40.90	68.14	<0.0001
	Chewiness	1152.44	1	1152.44	27.92	0.0011
C^2	Hardness	35.66	1	35.66	11.58	0.0144
	Springiness	2.25	1	2.25	63.65	<0.0001
	Adhesiveness	0.048	1	0.048	0.080	0.7858
	Chewiness	105.59	1	105.59	2.56	0.1538
A^2C	Hardness	197.17	1	197.17	64.04	0.0002
Residuals	Hardness	18.47	6	3.08	-	-
	Springiness	0.25	7	0.035	-	-
	Adhesiveness	4.20	7	0.60	-	-
	Chewiness	288.97	7	41.28	-	-
Lack of fit	Hardness	13.51	4	3.38	1.36	0.4650
	Springiness	0.19	5	0.038	1.29	0.4899
	Adhesiveness	3.47	5	0.69	1.89	0.3807
	Chewiness	285.81	5	57.16	36.20	0.0271

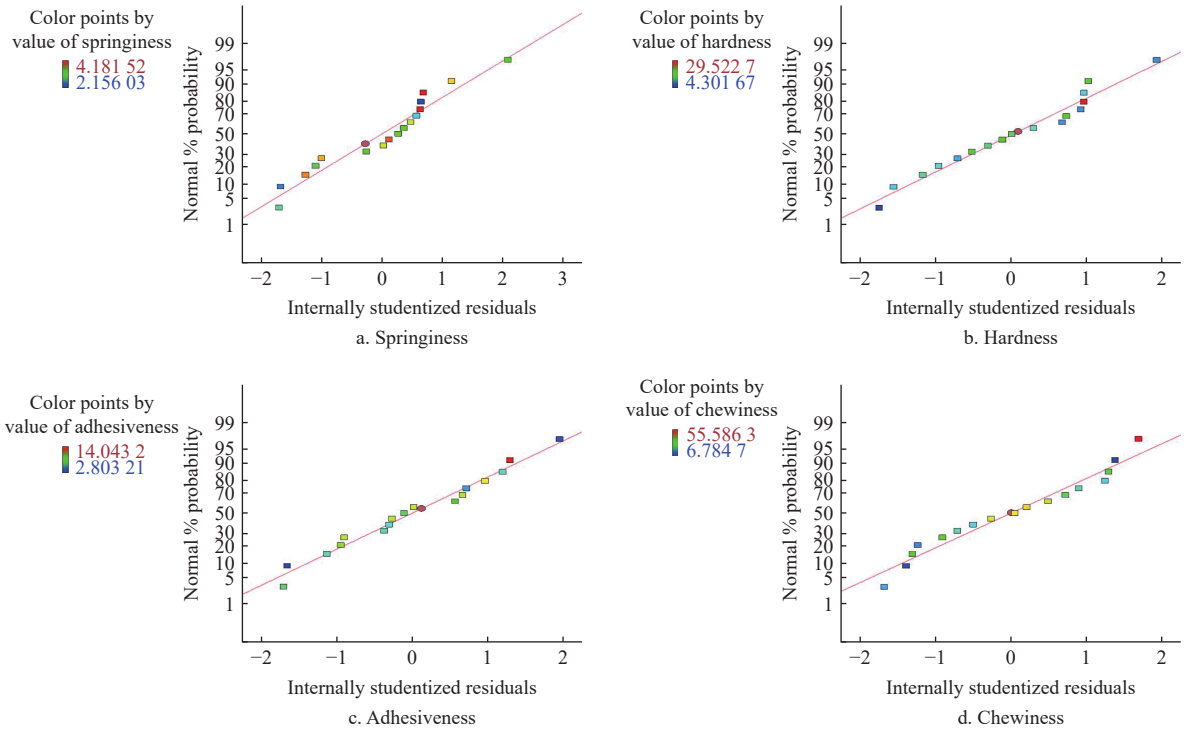

Figure 2 Normality plot of residuals for the midsection of the chicken feet tarsometatarsal bones

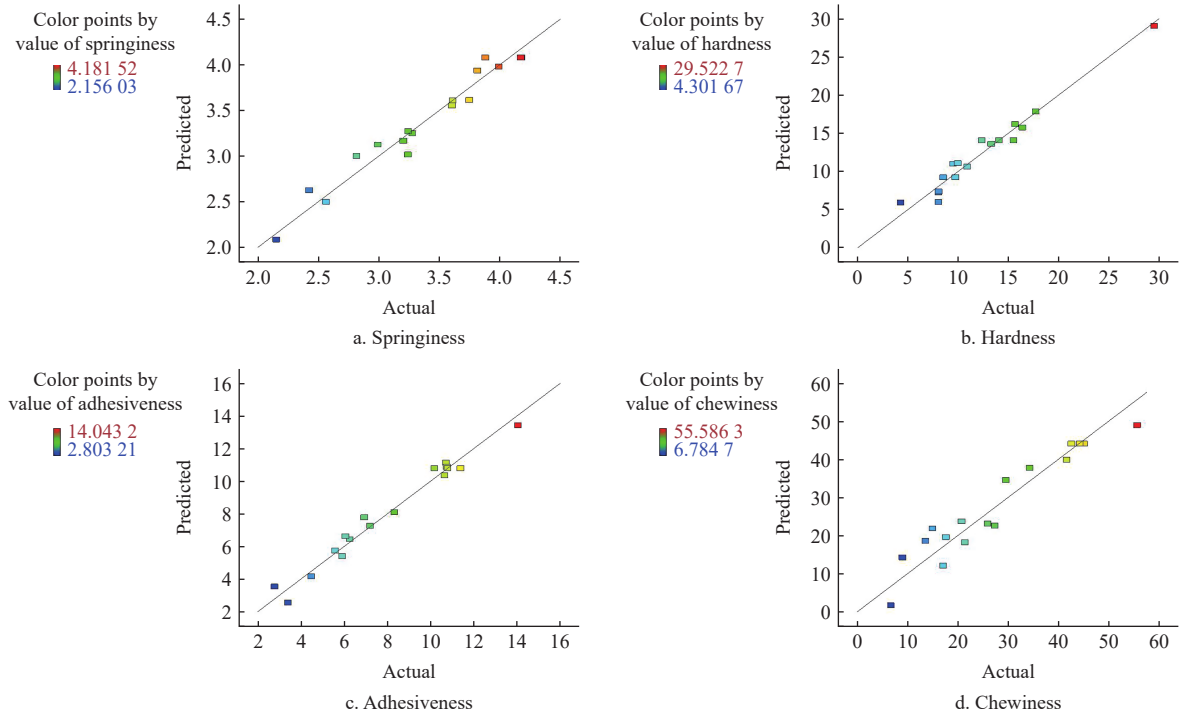

Figure 3 Comparison plot of the predicted and experimental values for the TPA regression equation of springiness, hardness, adhesiveness, and chewiness in the midsection of chicken feet tarsometatarsal bones

Table 4 Regression coefficients of the TPA response models

Response	Intercept	x_1/°C	x_2/min	x_3/°C	$x_1 \cdot x_2$	$x_1 \cdot x_3$	$x_2 \cdot x_3$	x_1^2	x_2^2	x_3^2	$x_1^2 x_3$
y_1/mm	–22.744 52	0.462 00	0.587 93	0.396 64	–0.003 37	–0.003 50	–0.003 74	–0.002 10	–0.011 18	–0.002 86	0.000 00
y_2/N	–1338.68354	30.266 83	5.655 21	85.424 46	–0.049 34	–1.942 40	–0.019 72	–0.169 12	–0.065 08	0.011 38	0.010 97
y_3/N	–253.905 94	5.270 14	4.864 14	1.770 79	–0.039 85	–0.016 79	–0.015 01	–0.026 87	–0.062 96	–0.000 42	0.000 00
y_4/mJ	–1182.01229	24.711 88	19.459 12	6.311 60	–0.135 22	–0.049 99	–0.076 77	–0.129 39	–0.334 24	–0.019 59	0.000 00

Note: x_1 is the heating temperature; x_2 is the heating time; x_3 is the cooling temperature. The response variables y_1, y_2, y_3, and y_4 represent springiness, hardness, adhesiveness, and chewiness, respectively.

affect peel strength. The influence of the heating temperature and heating time on the peel strength may be relatively small, whereas the influence of the cooling temperature is significant. The sum of squares for residuals is 0.32, indicating a good fit of the model. The

lack-of-fit F-value is 4.37, with a significance level of 0.2010, suggesting a nonsignificant lack of fit. Therefore, the model fits the data well, and a significant lack of fit is not indicated.

Table 5 Results of the peel test on the midsection of the chicken feet tarsometatarsal bones

Run	A: Heating temperature/°C	B: Heating time/min	C: Cooling temperature/°C	Peel strength/kN·m^{-1}
1	95.0	5.00	25.0	1.848
2	87.5	1.25	12.5	1.360
3	87.5	10.50	33.5	2.252
4	95.0	5.00	0.0	0.567
5	95.0	16.00	25.0	1.394
6	74.9	10.50	12.5	1.780
7	87.5	10.50	12.5	1.195
8	80.0	5.00	0.0	0.959
9	95.0	16.00	0.0	0.636
10	87.5	10.50	12.5	1.262
11	87.5	10.50	–8.5	0.519
12	80.0	16.00	25.0	1.644
13	87.5	19.75	12.5	0.832
14	80.0	5.00	25.0	2.073
15	80.0	16.00	0.0	0.626
16	100.0	10.50	12.5	0.770
17	87.5	10.50	12.5	1.102

Table 6 ANOVA results for peel strength

Source	Sum of squares	Degrees of freedom	Mean square	F-value	Significance
Model	4.46	3	1.490	60.00	<0.0001
A: Heating temperature/°C	0.48	1	0.480	19.31	0.0007
B: Heating time/min	0.30	1	0.300	12.25	0.0039
C: Cooling temperature/°C	3.68	1	3.680	148.44	<0.0001
Residuals	0.32	13	0.025	-	-
Lack of fit	0.31	11	0.028	4.37	0.2010

The R^2 value of 0.9326 suggests that factors such as heating temperature, heating time, and cooling temperature have a significant effect on peel strength and that increasing these values results in greater peel strength. Additionally, the adjusted coefficient of determination (adjusted R^2) of 0.9171 shows that the model remains highly accurate even after accounting for degrees of freedom. The adequate precision value of 22.861 further supports the model's reliability in predicting peel strength. The standard distribution plot of residuals for peel strength (Figure 4) shows a nearly linear distribution of data points along the diagonal, indicating that the regression model can explain most of the variation in peel strength and that the residuals approach a normal distribution.

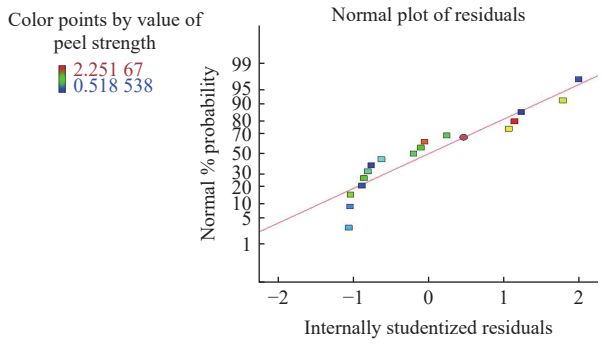

Figure 4 Standard distribution plot of the residuals for peel strength

The comparison of the predicted and experimental values (Figure 5) reveals a nearly linear distribution along the diagonal, indicating strong agreement between the predicted and actual values. The proximity of the data points to the diagonal suggests minimal deviations between the predicted and actual values, reflecting the high accuracy of the regression model.

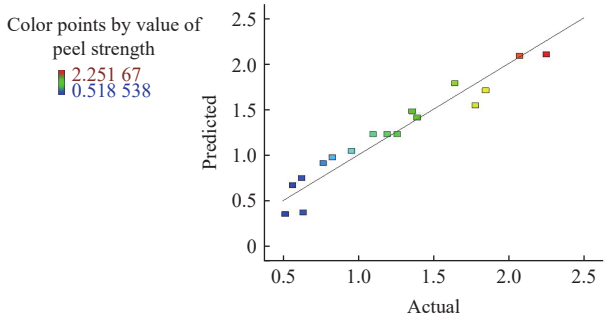

Figure 5 Comparison plot between the predicted values and experimental values of the peel strength regression equation

The regression equation strongly fits the peel strength data, as evidenced by the correlation metrics, adequate precision, regular distribution of residuals, and comparison between the predicted and experimental values. The model is able to explain a significant portion of the variation in peel strength, with minimal prediction errors and a strong linear relationship between the predicted and experimental values.

These findings indicate that the regression equation is highly effective in predicting peel strength. The equation, expressed in Equation (2), relates the independent variables (heating temperature, heating time, and cooling temperature) to the dependent variable (peel strength) as follows:

$$y_5 = 0.317\,000\,0 - 0.002\,495\,6x_1 - 0.002\,710\,5x_2 + 0.004\,151\,2x_3 \quad (2)$$

where, y_5 is the peel strength, kN/m; x_1 is the heating temperature, °C; x_2 is the heating time, min; and x_3 is the cooling temperature, °C.

The fluorescence imaging results provide microstructural evidence that the changes in peel strength are attributed to thermal denaturation, tissue restructuring, and stabilization during cooling. Proper processing facilitates peeling, while under- or over-treatment leads to incomplete softening or excessive compactness. Cooling plays a dominant role, likely due to moisture redistribution and protein re-association. These results agree with previous studies[31-33,38]. Importantly, this study quantitatively links peel strength with TPA parameters for process optimization.

3.3 Grid search

Based on the good agreement between the predicted and experimental values for both the TPA indicators and peel strength (Figures 3 and 5), the developed regression models were considered reliable for subsequent parameter optimization by grid search. The maximum score of the parameter model was 21.48, corresponding to the optimal combination of a cooling temperature of 5.0°C, a heating time of 8.00 min, and a heating temperature of 89.0°C. A total of 565 parameter combinations with scores greater than or equal to 20 were identified, with heating time ranging from 7.00 to 14.00 min, heating temperature from 84.0°C to 92.0°C, and cooling temperature from 0.0°C to 16.0°C. These results indicate a relatively broad processing window with stable overall performance.

As shown in Figure 6, higher-score parameter combinations

were mainly concentrated in the central region of the plot, whereas lower-score combinations were more sparsely distributed toward the periphery. This distribution suggests that the optimal parameter region was located near the center of the tested range.

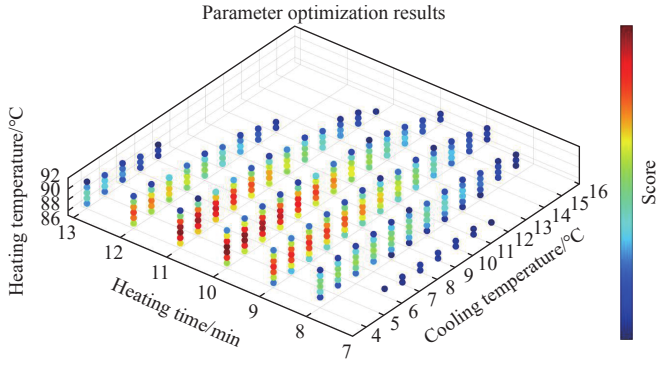

Figure 6 Parameter optimization scatter plot

3.4 Fluorescence imaging analysis

The fluorescence images of the treated samples stained with rhodamine B are presented in Figure 7. The selected samples represent different levels of the scoring model, with Figure 7b corresponding to the optimal condition and Figure 7d representing the lowest score. As highlighted by the red circles, the nonfluorescent regions exhibit distinct circular pore-like structures, whose size and distribution vary under different treatment conditions.

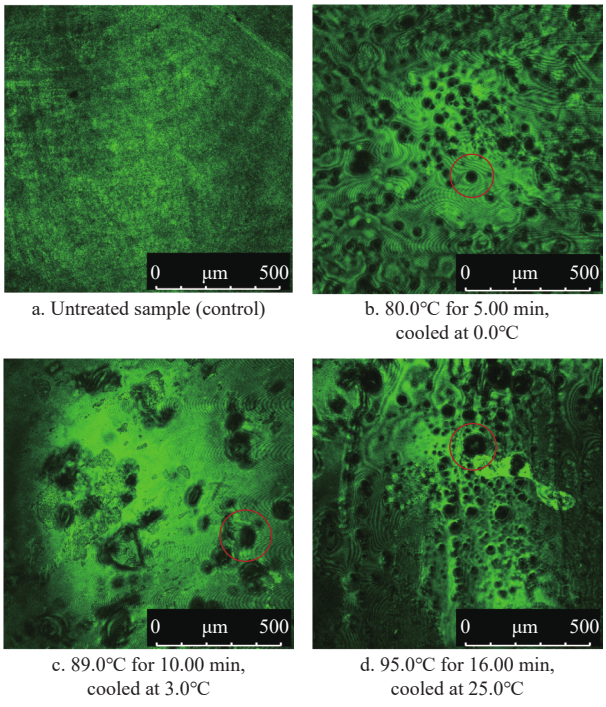

a. Untreated sample (control)

b. 80.0°C for 5.00 min, cooled at 0.0°C

c. 89.0°C for 10.00 min, cooled at 3.0°C

d. 95.0°C for 16.00 min, cooled at 25.0°C

Note: The red circles highlight representative nonfluorescent regions with circular pore-like structures, which are associated with protein aggregation and microstructural rearrangement. Differences in the size, distribution, and density of these regions reflect variations in protein denaturation and structural organization under different treatments.

Figure 7 Fluorescence imaging of chicken feet samples under different treatment conditions

The fluorescent and nonfluorescent parts of Figure 7a exhibited a uniform, dot-like distribution. This could indicate that the protein molecules are not adequately bound to each other, preventing denaturation and coalescence. Consequently, the muscle fibers in chicken feet are softer, and the connections between them are weaker. The nonfluorescent parts of both Figure 7b and Figure 7d are circular in shape. The distribution of circular pores in Figure 7d is denser than that in Figure 7b, and the diameter of the circular pores in Figure 7d is larger than that in Figure 7b. This may indicate excessive denaturation and coalescence of the protein in Figure 7d, resulting in overly tight cross-links between protein molecules, which can make the muscle fibers of the chicken feet stiff and sticky, affecting their texture and chewiness. The presence of irregularly shaped, highly fluorescent parts in Figure 7d also indicates excessive coalescence of the protein.

The large nonfluorescent parts in Figure 7c constitute a significantly smaller proportion of the total area. The nonfluorescent parts are irregularly shaped and evenly distributed. The coalescence of the nonfluorescent parts in Figure 7c may indicate moderate denaturation, coagulation, and cross-linking of the proteins. Despite this, the treatment conditions are conducive to maintaining the tenderness of the muscle fibers, ensuring good taste and maturity of the chicken feet.

The untreated chicken feet, serving as the control group, are depicted in Figure 7a. Figure 7b shows samples treated at a heating temperature of 80.0°C for 5.00 min and then cooled at 0.0°C. Figure 7c represents samples subjected to a heating temperature of 89.0°C for 10.00 min, followed by cooling at 3.0°C. Finally, Figure 7d illustrates samples treated at a higher heating temperature of 95.0°C for 16.00 min and cooled at 25.0°C. All samples were stained with rhodamine B to enable fluorescence imaging.

The fluorescence imaging results provide microstructural evidence supporting the observed differences in peel strength and TPA parameters. Samples with uniformly distributed nonfluorescent regions exhibited a better balance between peeling performance and texture quality, suggesting that moderate protein denaturation and cross-linking are beneficial. In contrast, overly dense regions indicate excessive aggregation and structural stiffening, which may negatively affect tenderness and chewiness. Overall, these results confirm that macroscopic texture and peel strength are closely associated with microstructural reorganization under different processing conditions.

4 Conclusions

This study developed a novel process optimization framework for chicken feet tarsometatarsal bones by integrating peel strength constraints with texture profile analysis (TPA) and implementing a grid search strategy. Unlike conventional approaches that focus on single quality attributes, the proposed method enables the simultaneous evaluation and optimization of mechanical properties and textural characteristics. The optimal processing condition (cooling at 5.0°C, heating for 8.00 min, and heating at 89.0°C) achieved the best overall performance, while a relatively broad and stable processing window was also identified, demonstrating the robustness of the approach. Among the examined factors, cooling temperature exhibited a more pronounced influence on peel strength than heating time and heating temperature, highlighting the critical role of thermal history in regulating protein structural transitions and moisture redistribution. In addition, the selected processing parameters significantly affected key textural attributes, including hardness, springiness, adhesiveness, and chewiness, confirming their comprehensive impact on product quality. Overall, this study not only provides a quantitative and mechanistically informed strategy for optimizing deboning conditions, but also offers a novel

perspective for integrating multi-attribute quality evaluation in poultry processing, with practical implications for improving processing efficiency and product standardization.

Acknowledgements:

This research was supported by the National Key R&D Program of China (2023YFD2101001).

[References]

[1] Ratna, Ulfariati C, Yusmanizar, Aprilia S, Rahmiati, Munawar A A. Development of biocomposite edible film food packaging based on gelatin from chicken claw waste. Case Stud Chem Environ Eng, 2023; 8: 100371.

[2] Deng G Y, Jiang X C, Song Z H, Li C M, Guan Y P, Guo S W, et al. Authentication of chicken-derived components in collagen-containing foods using natural macromolecular marker fragments by LC-MS method. Polym Test, 2023; 120: 107950.

[3] Kaewbangkerd K, Hamzeh A, Yongsawatdigul J. Ultrasound-assisted extraction of collagen from broiler chicken trachea and its biochemical characterization. Ultrason Sonochem, 2023; 95: 106372.

[4] Nassar F S. Chicken feet reimagined: A strategic platform for nutritional innovation, industrial valorization, and academic-industry synergies. Poult Sci, 2026; 105(7): 106888.

[5] Oyom W, Awuku R B, Faraji H, Bi Y, Tahergorabi R. Protein hydrogel formation from chicken processing by-products: Exploring applications in food. Food Res Int, 2025; 201: 115632.

[6] Gao D M, Xu W Y. The peeling characteristics and affected factors of chicken feet tarsometatarsus. Journal of Chinese Institute of Food Science and Technology, 2024; 24(7): 278–285. (in Chinese)

[7] Riggs M R, Hauck R, Baker-Cook B I, Osborne R C, Pal A, Terra M T B, et al. Meat quality of broiler chickens processed using electrical and controlled atmosphere stunning systems. Poult Sci, 2023; 102(3): 102422.

[8] Ramírez A C E, Hurtado-Macías A, Talamantes R, Flores E, Ladrón De Guevara H P, Delgado J I, et al. Assessing mechanical behavior of ostrich and equine trabecular and cortical bone based on depth sensing indentation measurements. J Mech Behav Biomed Mater, 2021; 117: 104404.

[9] Carril J, Barbeito C G, Tambussi C P. Making a parrot zygodactyl foot: Osteology and morphogenesis of the tarsometatarsus in the monk parakeet (*Myiopsitta monachus*). Zoology, 2021; 144: 125877.

[10] Bell A, Wu Y H, Chiapp L M. Morphometric comparison of the Hesperornithiformes and modern diving birds. Palaeogeogr Palaeoclimatol Palaeoecol, 2019; 513: 196–207.

[11] Chen C S, Jiang S Y, Li M F, Li Y, Li H, Zhao F, et al. Effect of high temperature cooking on the quality of rice porridge. Int J Agric Biol Eng, 2021; 14: 247–54.

[12] Tura M, Gagliano M A, Valli E, Petracci M, Gallina T T. A methodological review in sensory analyses of chicken meat. Poult Sci, 2024; 103: 104083.

[13] Liu C, Li Y L, Sun W M, Ma F Y, Wang X W, Yang Z H. New techniques of meat quality assessment for detecting meat texture. Processes, 2025; 13(3): 640.

[14] Rahman M S, Al-Farsi S A. Instrumental texture profile analysis (TPA) of date flesh as a function of moisture content. J Food Eng, 2005; 66: 505–511.

[15] Amatya I, Seo J, Letcher T, Ahn J H. Peel and cleavage strength tests with adhesive connections in dynamic message signs. Int J Adhes Adhes, 2020; 103: 102715.

[16] Pillet B, Badel P, Pierrat B. Effects of cryo-preservation on skeletal muscle tissues mechanical behavior under tensile and peeling tests until rupture. J Mech Behav Biomed Mater, 2022; 132: 105273.

[17] García-Segovia P, Andrés-Bello A, Martínez-Monzó J. Textural properties of potatoes (*Solanum tuberosum* L., cv. Monalisa) as affected by different cooking processes. J Food Eng, 2008; 88(1): 28–35.

[18] Meziani S, Jasniewski J, Ribotta P, Arab-Tehrany E, Muller J M, Ghoul M, et al. Influence of yeast and frozen storage on rheological, structural and microbial quality of frozen sweet dough. J Food Eng, 2012; 109: 538–544.

[19] Dolores Romero De Ávila M, Isabel Cambero M, Ordóñez J A, De La Hoz L, Herrero A M. Rheological behaviour of commercial cooked meat products evaluated by tensile test and texture profile analysis (TPA). Meat Sci, 2014; 98(2): 310–315.

[20] Peng F, Huang Z G, Fang F. Modeling and experiments of chewing mechanical properties of pellet feed using discrete element method. Int J Agric Biol Eng, 2020; 13(4): 37–44.

[21] Zushi K, Higashijima M. Correlation network analysis identified the key interactions of texture profiles with the sensory, physical, and organoleptic properties of cherry tomato cultivars grown under salt stress. Sci Hortic, 2022; 293: 110754.

[22] Pillet B, Badel P, Edouard P, Pierrat B. Hamstring muscles rupture under traction, peeling and shear lap tests: A biomechanical study in rabbits. J Mech Behav Biomed Mater, 2021; 116: 104324.

[23] Bartlett M D, Case S W, Kinloch A J, Dillard D A. Peel tests for quantifying adhesion and toughness: A review. Prog Mater Sci, 2023; 137: 101086.

[24] Wei Y, Jin X H, Luo Q T, Li Q, Sun G Y. Adhesively bonded joints – A review on design, manufacturing, experiments, modeling and challenges. Compos Part B Eng, 2024; 276: 111225.

[25] Zhou P, Li H P, Chai T Y. SPEA2 based on grid density search and elite guidance for multi-objective operation optimization of wastewater treatment process. App.Soft Comput, 2023; 144: 110529.

[26] Vega P, Revollar S, Francisco M, Martín J M. Integration of set point optimization techniques into nonlinear MPC for improving the operation of WWTPs. Comput Chem Eng, 2014; 68: 78–95.

[27] Ghorbani Mooselu M, Nikoo M R, Latifi M, Sadegh M, Al-Wardy M, Al-Rawas G A. A multi-objective optimal allocation of treated wastewater in urban areas using leader-follower game. J Clean Prod, 2020; 267: 122189.

[28] Perrignon M, Croguennec T, Jeantet R, Emily M. The multi-objective data-driven approach: A route to drive performance optimization in the food industry. Trends Food Sci Technol, 2024; 152: 104697.

[29] Boateng I D. Application of graphical optimization, desirability, and multiple response functions in the extraction of food bioactive compounds. Food Eng Rev, 2023; 15: 309–328.

[30] Chitsaz S, Tarighat A. Estimation of the modulus of elasticity of N-A-S-H and slag-based geopolymer structures containing calcium and magnesium ions as impurities using molecular dynamics simulations. Ceram Int, 2021; 47(5): 6424–6433.

[31] Li X F, Chen L Y, Hua Y F, Chen Y M, Kong X Z, Zhang C M. Effect of preheating-induced denaturation during protein production on the structure and gelling properties of soybean proteins. Food Hydrocoll, 2020; 105: 105846.

[32] Kyomugasho C, Wainaina I, Grauwet T, Van Loey A, Hendrickx M E. Bean softening during hydrothermal processing is greatly limited by pectin solubilization rather than protein denaturation or starch gelatinization. Food Res Int, 2023; 165: 112471.

[33] Li R L, Wu N, Xue H, Gao B H, Liu H L, Han T F, et al. Influence and effect mechanism of disulfide bonds linkages between protein-coated lipid droplets and the protein matrix on the physicochemical properties, microstructure, and protein structure of ovalbumin emulsion gels. Colloids Surf B Biointerfaces, 2023; 223: 113182.

[34] Frabetti A C C, De Moraes J O, Jury V, Boillereaux L, Laurindo J B. Adhesion of food on surfaces: Theory, measurements, and main trends to reduce it prior to industrial drying. Food Eng Rev, 2021; 13: 884–901.

[35] Yuan X L, Zhang Z Y, Lin H B, Ye Y, Li A J. Physicochemical properties, microstructure and protein characteristic of frozen chicken feet as affected by different thawing methods. Int J Food Prop, 2023; 26: 1506–21.

[36] Gokul Nath K, Pandiselvam R, Sunil C K. High-pressure processing: Effect on textural properties of food- A review. J Food Eng, 2023; 351: 111521.

[37] Liu B, Liu Z Q, Li D Y, Yu M M, Liu Y X, Qin L, et al. Action of endogenous proteases on texture deterioration of the bay scallop (*Argopecten irradians*) adductor muscle during cold storage and its mechanism. Food Chem, 2020; 323: 126790.

[38] Lin M C, Lou C W, Lin J Y, Lin T A, Lin J H. Mechanical property evaluations of flexible laminated composites reinforced by high-performance Kevlar filaments: Tensile strength, peel load, and static puncture resistance. Compos Part B Eng, 2019; 166: 139–147.